Universal Distributions for Growth Processes in 1 + 1 Dimensions and Random Matrices

Michael Prähofer* and Herbert Spohn†

Zentrum Mathematik and Physik Department, TU München, D-80290 München, Germany

(Received 14 December 1999)

We develop a scaling theory for Kardar-Parisi-Zhang growth in one dimension by a detailed study of the polynuclear growth model. In particular, we identify three universal distributions for shape fluctuations and their dependence on the macroscopic shape. These distribution functions are computed using the partition function of Gaussian random matrices in a cosine potential.

PACS numbers: 64.60.Ht, 05.40.–a, 68.35.Ct, 81.10.Aj

Growth processes lead to a rich variety of macroscopic patterns and shapes [1]. As has been recognized for some time, growth may also give rise to intriguing statistical fluctuations comparable to thermal fluctuations at a critical point. One of the most prominent examples is the Kardar-Parisi-Zhang (KPZ) universality class [2]. In essence one models a stable phase which grows into an unstable phase through aggregation, as, for example, in Eden-type models where perimeter sites of a given cluster are filled up randomly. In real materials, mere aggregation is often too simplistic an assumption and one would have to take other dynamical modes, such as surface diffusion, at the stable/unstable interface into account [3]. In our Letter we remain within the KPZ class.

From the beginning there has been evidence that in one spatial dimension KPZ growth processes are linked to exactly soluble models of two-dimensional statistical mechanics. Kardar [4] mapped growth to the directed polymer problem. The replica trick then yields the Bose gas with attractive δ interaction which in one dimension can be solved through the Bethe ansatz [5]. In [6], considerably generalized in [7], for a particular discrete growth model the statistical weights for the local slopes were mapped onto the six vertex model. To solve the six vertex model one diagonalizes the transfer matrix, again, through the Bethe ansatz, which also allows for a study of finite size scaling [8]. Unfortunately none of these methods goes beyond what corresponds to the free energy in the six vertex model and the associated dynamical scaling exponent $\beta = 1/3$.

In this Letter we point out that within the KPZ universality class the polynuclear growth (PNG) model plays a distinguished role: it maps onto random permutations, the height being the length of the longest increasing subsequence of such a permutation, and thereby onto Gaussian random matrices [9,10]. We use these mappings to obtain an analytic expression for certain scaling distributions, which then leads to an understanding of how the self-similar height fluctuations depend on the initial conditions and to a more refined scaling theory for KPZ growth.

PNG is a simplified model for layer by layer growth [1]. One starts with a perfectly flat crystal in contact with its supersaturated vapor. Once in a while a supercritical nucleus is formed, which then spreads laterally by further attachment of particles at its perimeter sites. Such islands coalesce if they are in the same layer and further islands may be nucleated upon already existing ones. The PNG model ignores the lateral lattice structure and assumes that the islands are circular and spread at constant speed. The nucleation rate and the lateral speed can be set to one by the appropriate choice of space-time units.

We specialize to a one-dimensional surface, returning to higher dimensions at the end. The height, $h(x,t)$, at time t above the point x on the substrate is counted in lattice spacings. The upward steps of h move deterministically with velocity -1, the downward steps with velocity $+1$, and they annihilate upon touching. Through a nucleation event at (x,t), randomly in space-time, h increases at x by one unit thereby creating a new up-down pair of steps. To explain the mapping from PNG to permutations it is convenient to first use a droplet geometry, where a single island starts spreading from the origin and further nucleations take place only above this ground layer. The initially flat substrate and other initial conditions will be handled along the lines of this blueprint.

We want to compute the height $h(x,t)$ of the droplet. Clearly it is determined by the set of nucleation events inside the rectangle $R_{(x,t)} = \{(x',t'): |x'| \le t' \text{ and } |x - x'| \le t - t'\}$. In lightlike coordinates, $r = (t' + x')/\sqrt{2}$, $s = (t' - x')/\sqrt{2}$, the rectangle $R_{(x,t)}$ equals $[0,R] \times [0,S]$ with $R = (t + x)/\sqrt{2}$, $S = (t - x)/\sqrt{2}$. We label the nucleation events as (r_n, s_n), $n = 1, \ldots, N$, such that $0 \le r_1 < \cdots < r_N \le R$. The corresponding order in the second coordinate s, $0 \le s_{p(1)} < \cdots < s_{p(N)} \le V$, defines then a permutation p of length N; compare with Fig. 1.

There is a simple rule of how to determine the number of the layer in which each nucleation event is located. Points in layer 1 are obtained by scanning the permutation $[p(1), \ldots, p(N)]$ from left to right and marking all those entries which are smaller than the so far smallest. After deleting the subsequence of the first layer, the second layer is obtained by repeating this construction. One marks those of the remaining entries of the permutation which are in decreasing order. At the end the permutation p has been subdivided into decreasing subsequences. In the example of Fig. 1 we have the permutation $(4, 7, 5, 2, 8, 1, 3, 6)$. The

 0031-9007/00/84(21)/4882(4)$15.00

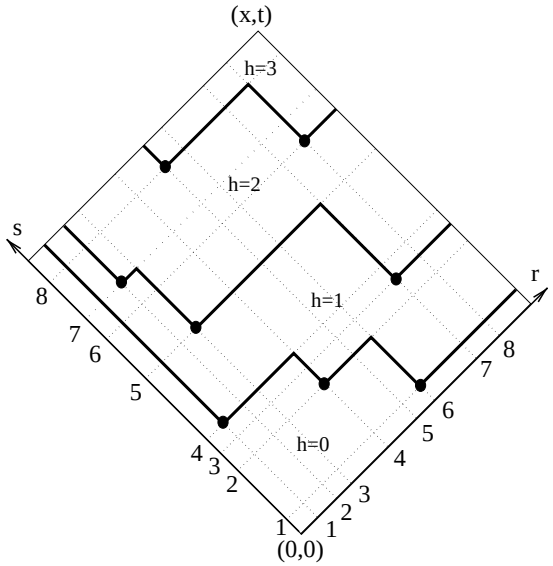

FIG. 1. The height h of a PNG droplet with nucleation events corresponding to the permutation $(4, 7, 5, 2, 8, 1, 3, 6)$.

first decreasing subsequence is $(4, 2, 1)$, corresponding to the nucleation events in the first layer. The remaining subsequences are $(7, 5, 3)$ and $(8, 6)$. The height $h(x, t)$ is the number of these subsequences and therefore the length of the longest increasing subsequence of p [10].

In a dual picture one draws a directed path from $(0, 0)$ to (x, t), joining nucleation events by straight lines, with the restriction that both coordinates r and s are increasing along the path. Equivalently, the path must be in the forward light cone at each nucleation event. This is the celebrated directed polymer, cf., for example, [1], in the context of the PNG model. If to each path we assign as negative energy the number of nucleation centers traversed, then $h(x, t)$ equals the ground state energy of the directed polymer. The PNG model is thus in the strong coupling regime.

The nucleation events have density one and are independently and uniformly distributed in the rectangle $R_{(x,t)}$ with area $\lambda = (t^2 - x^2)/2$. This induces a Poisson distribution for the length, N, of the permutation, $\mathrm{Prob}\{N = n\} = e^{-\lambda}\lambda^n/n!$, and for a given length n each permutation has the same probability, namely, $1/n!$. Thus the problem of computing the distribution of the height $h(x, t)$ is converted into determining the statistics of the length, l, of a longest increasing subsequence of a random permutation. Since to leading order $h(x, t) \propto t$, l must be of order $\sqrt{\lambda}$ and the relative fluctuations should be of order $\lambda^{1/6}$, if we accept $\beta = 1/3$ for KPZ growth in the $1 + 1$ dimension.

The same construction can be carried out for an initially flat substrate. By translation invariance, it suffices to study $H(t) = h(0, t)$. The rectangle $R_{(0,t)}$ is now replaced by the triangle $T_t = \{(x', t') : |x'| \le t - t', t' \ge 0\}$. To relate to the directed polymer we add the mirror image relative to $t = 0$, including the nucleation events, to obtain the square $R_t = \{(x', t') : |x'| \le t - |t'|\}$. Then $2H(t)$ equals again the ground state energy of the directed polymer from $(0, -t)$ to $(0, t)$. However, the statistics of nucleation centers inside R_t is constrained to satisfy the reflection symmetry relative to $t = 0$.

For a random permutation with Poisson distributed length N, $\langle N \rangle = \lambda$, the length l of the longest increasing subsequence satisfies the amazing identity

$$\mathrm{Prob}\{l \le m\} = e^{-\lambda} \int_{m \times m} dU \exp[\sqrt{\lambda}\,\mathrm{Tr}(U + U^{-1})], \tag{1}$$

where the integration is uniformly over all $m \times m$ unitary matrices. A proof can be found, for example, in [10,11]. The partition function in (1) appeared before in the context of quantum gravity and has a third order phase transition at $m \simeq 2\sqrt{\lambda}$ with finite size scaling governed by the Painlevé II equation [12,13]. Baik *et al.* [11] prove that $l \simeq 2\sqrt{\lambda} + \lambda^{1/6}\chi_2$ for large λ, where χ_2 is a random variable distributed according to the GUE Tracy-Widom distribution, i.e., the distribution of the largest eigenvalue of a complex Hermitian random matrix [14]. One has $\mathrm{Prob}\{\chi_2 \le x\} = F_2(x) = e^{-g(x)}$, where $g''(x) = \mathrm{u}(x)^2$, $g(x) \to 0$ as $x \to \infty$, and $\mathrm{u}(x)$ is the global positive solution of the Painlevé II equation $\mathrm{u}'' = 2\mathrm{u}^3 + x\mathrm{u}$. Its asymptotics are $\mathrm{u}(x) \sim \sqrt{-x/2}$ for $x \to -\infty$ and $\mathrm{u}(x) \sim \mathrm{Ai}(x)$ for $x \to \infty$, $\mathrm{Ai}(x)$ the Airy function.

To translate to the PNG model we introduce the growth velocity $v(u)$, depending on the macroscopic slope $u = \partial h/\partial x$, and the static roughness $A(u)$ [15], which for PNG are $v(u) = \sqrt{2 + u^2}$, $A(u) = \sqrt{2 + u^2}$ in our units. Then

$$h(-v'(u)t, t) \simeq [v(u) - uv'(u)]t + [\tfrac{1}{2}v''(u)A(u)^2 t]^{1/3}\chi_2 \tag{2}$$

in the limit of large t. We emphasize that all nonuniversal factors are given through the model dependent quantities $v(u)$, $A(u)$ and remark that (2) is also confirmed by the rigorous result of Johansson [16] for a discrete growth model equivalent to the totally asymmetric simple exclusion process.

For the flat substrate one might expect to have the same fluctuation law as for the droplet, since in both cases the mean curvature vanishes on a microscopic scale. A result of Baik and Rains [17] tells us, however, that the fluctuations are GOE [14]. More precisely, there is a similar formula for $\mathrm{Prob}\{l \le m\}$ as (1) in the case that the random permutation p is reflection symmetric relative to the antidiagonal, $p(N + 1 - p(k)) = N + 1 - k$. The asymptotic analysis of [17] results in $l \simeq 4\sqrt{\lambda} + (2\lambda)^{1/6}\chi_1$, where χ_1 is distributed as the largest eigenvalue of a real symmetric random matrix. Translated to the surface this means

$$H(t) = \sqrt{2}\,t + (t/\sqrt{2})^{1/3}\chi_1\,. \tag{3}$$

One has $\mathrm{Prob}\{2^{2/3}\chi_1 \le x\} = F_1(2^{-2/3}x) = e^{-[f(x)+g(x)]/2}$,

$g(x)$ as above and $f'(x) = -u(x)$, $f(x) \to 0$ for $x \to \infty$. The distributions of χ_2 and χ_1 are plotted in Fig. 2. Superimposed are Monte Carlo data for the PNG model, which differ distinguishably from the analytical curves only at the tails where statistics becomes bad. We conclude that the droplet and the flat substrate have the same scaling form but distinct universal distributions.

The flat substrate, although used in many simulations, and the droplet are rather special as initial conditions. From a statistical mechanics point of view stationary growth would be regarded as singled out, which for PNG corresponds to initial conditions where the up and down steps are random with densities $\sqrt{2}$ each. Physically, another natural initial condition is to have a staircase configuration representing a tilted surface. In addition we could have sources, for example, additional nucleation events at the origin. The mapping to the directed polymer works as before. Our crucial observation is that such other initial conditions translate in essence to defect lines and/or boundary potentials for the directed polymer.

To illustrate, we discuss only one special geometry. As for the droplet we consider random nucleations of density one in the square $R_{(0,t)}$. In addition there are random nucleations at the two lower edges $\{s = 0\}$ and $\{r = 0\}$ with constant line densities ρ_+ and ρ_-, respectively. Thus the path of minimal energy, with starting point at $(0, 0)$, sticks for a while at one of the two edges and then enters the bulk to reach $(0, t)$ eventually. If $\rho_+ < 1$, $\rho_- < 1$, it does not pay to stay at the edges, and from the bulk we have GUE energy fluctuations according to (2). On the other hand if $\rho = \max\{\rho_+, \rho_-\} > 1$, the optimal path stays for a length $t(1 - 1/\rho^2)/\sqrt{2}$ at the edge with the higher density. Since the edge events are random, the $t^{1/3}$ bulk fluctuations are dominated by the Gaussian $\sqrt{t}$ edge fluctuations. Parenthetically we remark that for regularly spaced edge points one should recover GOE.

The length distribution along the critical lines $\rho_+ = 1$, $\rho_- < 1$, and $\rho_+ < 1$, $\rho_- = 1$, was identified by Baik and Rains [18], in a generalization of the techniques in [17]. They obtain GOE^2 fluctuations, i.e., the distribution of the maximum of two independent GOE random variables. The path of minimal energy stays for a length of order $t^{1/3}$ at the density one edge. At the critical point $\rho_+ = \rho_- = 1$, the polymer has a choice between the left and right edge. By a limiting procedure one obtains [18] the universal distribution for the energy fluctuations, $F_0(x) = \mathrm{Prob}\{\chi_0 < x\}$, with

$$F_0(x) = [1 - (x + 2f'' + 2g'')g']e^{-(g+2f)}. \quad (4)$$

An interpretation in terms of the eigenvalue distribution of random matrices has yet to be found. In Fig. 2 we plot the distribution of χ_0. Superimposed are simulation data for the PNG model, taken before the analytic result had been obtained. The first four moments of χ_j, $j = 0, 1, 2$, are listed in Table I. Of interest are also the asymptotics of the probability densities $F_j'(x)$. From Painlevé II we obtain $-\log F_j'(x) = c_j|x|^3/12$ for $x \to -\infty$ and $-\log F_j'(x) = d_j x^{3/2}/3$ for $x \to \infty$ up to logarithmic corrections with prefactors $c_j = 1, 2, 1$ and $d_j = 2, 4, 4$ for $j = 0, 1, 2$, respectively.

We have to translate back to surface growth. For stationary growth with zero slope, in the space-time picture, the height lines cross the forward light cone with the densities $\rho_+ = 1 = \rho_-$ and the intersection points are Poisson distributed [20]. Thus for the directed polymer with edge densities the critical point is precisely stationary growth with zero slope. If $\rho_+\rho_- = 1$, $\rho_+ \neq 1$, we have also stationary growth but now with slope $u = (\rho_- - \rho_+)/\sqrt{2}$. As argued already the fluctuations along the line $x = 0$ are then Gaussian $\sqrt{t}$. For the $t^{1/3}$ fluctuations one has to record height differences along the line $\{x = v'(u)t\}$, as can be seen from a similarity transformation. In Fig. 3 we illustrate the macroscopic shape for general boundary sources. If $\rho_+ = 0 = \rho_-$, we have the droplet discussed before. Nonzero boundary sources enforce flat segments tangential to the droplet shape. The profile at $x = 0$ is curved for $\rho_+ < 1$, $\rho_- < 1$, flat otherwise, the marginal case corresponding to the critical lines.

Our detailed study of the PNG model suggests the following scaling theory for all growth models in the KPZ universality class. First of all we require a self-similar macroscopic shape. Locally this leaves only two possibilities, either a flat piece or a curved piece with a shape determined through the slope dependent growth velocity

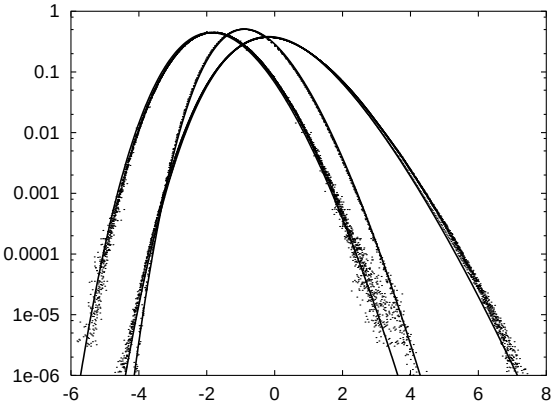

FIG. 2. From left to right: the probability densities of the universal distributions χ_2, χ_1, and χ_0 for curved, flat, and stationary self-similar growth, respectively.

TABLE I. Mean, variance, skewness, and kurtosis for the distributions of χ_2, χ_1, and χ_0 as determined by numerically solving Painlevé II [19]. $\langle \chi^n \rangle_c$ denotes the nth cumulant.

	Curved (χ_2)	Flat (χ_1)	Stationary (χ_0)
$\langle \chi \rangle$	−1.771 09	−0.760 07	0
$\langle \chi^2 \rangle_c$	0.813 20	0.638 05	1.150 39
$\langle \chi^3 \rangle_c / \langle \chi^2 \rangle_c^{3/2}$	0.2241	0.2935	0.359 41
$\langle \chi^4 \rangle_c / \langle \chi^2 \rangle_c^2$	0.093 45	0.1652	0.289 16

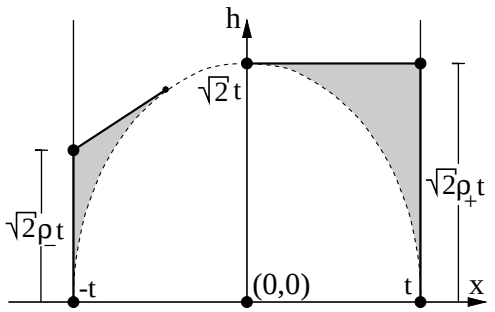

FIG. 3. Droplet with boundary sources of intensity $\rho_- < 1$ and $\rho_+ = 1$ (critical). The dashed line corresponds to the free droplet. The shaded region is the extra mass due to sources.

[21]. We draw a ray from the center of symmetry. If the surface at the point of intersection with the ray has nonzero curvature, then the height fluctuations in this direction are GUE with scaling form (2). If the curvature is zero, we have to know the roughness of the initial conditions, i.e., $|h(x,0) - h(0,0)| \propto |x|^\alpha$ with roughness exponent α, and/or the corresponding roughness for boundary sources. If $\alpha = 0$ the height fluctuations are GOE and the general scaling form is as in (2) with χ_2 replaced by χ_1. If $\alpha = 1/2$ the height fluctuations are Gaussian with variance proportional to t, except along the line $\{x = v'(u)t\}$, where they again have the scaling form (2) with the random variable χ_2 replaced by χ_0, as defined in (4). The intermediate cases $0 < \alpha < \frac{1}{2}$ have not been studied systematically. Also the fluctuations at the end points of flat pieces have still to be classified. There are two exceptions. One is the case of Fig. 3, which has GOE^2 and the second one is the half-droplet with an external source at $x = 0$. Translating [17] to PNG one finds GOE, GSE, and Gaussian depending on the strength of the source.

Our constructions carry over immediately to higher dimensions, as can be seen most directly in the polymer picture. The square is replaced by a $(d+1)$-dimensional (hyper)cube with uniformly distributed nucleation centers, the polymer running from the lower to the upper tip. For the PNG model this corresponds to droplet growth with islands having the shape of a regular simplex (a triangle in $2+1$, a tetrahedron in $3+1$, and so on). One axis of the cube defines the order $1,\ldots,N$, while the remaining d axes define the permutations $p_i(1),\ldots,p_i(N)$, $i = 1,\ldots,d$. Increasing means now increasing in all coordinates, i.e., $j < j'$ and $p_i(j) < p_i(j')$ for all $1 \le i \le d$. The length of the longest increasing subsequence equals, again, the height of the droplet. At present we study numerically the statistics of this length with the goal to have information on scaling more precise than the one of previous investigations [22].

In conclusion, we have obtained distinct scaling functions for the PNG model, which depend on the choice of initial conditions. By universality we argued that from the knowledge of the self-similar curvature one can infer the type of height fluctuations. It would be of interest to study also joint probability distributions of the height at distinct space-time points. Perhaps such a program could identify the universal field theory hiding behind KPZ growth in one dimension.

We are grateful to J. Baik and E. M. Rains for making their results [18] available to us prior to publication and to C. Tracy for help on Painlevé II.

*Email address: praehofer@ma.tum.de
†Email address: spohn@ma.tum.de

[1] P. Meakin, *Fractals, Scaling, and Growth Far From Equilibrium* (Cambridge University Press, Cambridge, England, 1998).
[2] M. Kardar, G. Parisi, and Y.-C. Zhang, Phys. Rev. Lett. **56**, 889 (1986).
[3] J. Krug, Adv. Phys. **46**, 139 (1997).
[4] M. Kardar, Nucl. Phys. **B290**, 582 (1987).
[5] E. H. Lieb and W. Liniger, Phys. Rev. **130**, 1605 (1963).
[6] L.-H. Gwa and H. Spohn, Phys. Rev. Lett. **68**, 725 (1992); Phys. Rev. A **46**, 844 (1992).
[7] D. Kim, Phys. Rev. E **52**, 3512 (1995).
[8] B. Derrida and J. L. Lebowitz, Phys. Rev. Lett. **80**, 209 (1998); B. Derrida and C. Appert, J. Stat. Phys. **94**, 1 (1999).
[9] E. M. Rains, Electron. J. Combin. **5**, R12 (1998).
[10] D. Aldous and P. Diaconis, Bull. Am. Math. Soc. **36**, 413 (1999).
[11] J. Baik, P. Deift, and K. Johansson, J. Am. Math. Soc. **12**, 1119 (1999).
[12] D. J. Gross and E. Witten, Phys. Rev. D **21**, 446 (1980).
[13] V. Periwal and D. Shevitz, Phys. Rev. Lett. **64**, 1326 (1990).
[14] C. A. Tracy and H. Widom, Commun. Math. Phys. **159**, 151 (1994); **177**, 727 (1996). The GUE, GOE, and GSE Tracy-Widom distributions arise there for the Gaussian unitary, orthogonal, and symplectic ensemble, respectively.
[15] M. Prähofer and H. Spohn, Physica (Amsterdam) **279A**, 342 (2000).
[16] K. Johansson, Commun. Math. Phys. **209**, 437 (2000).
[17] J. Baik and E. M. Rains, e-print math.CO/9910019.
[18] J. Baik and E. M. Rains, e-print math.PR/0003130.
[19] C. A. Tracy and H. Widom, e-print solv-int/9707001.
[20] D. Aldous and P. Diaconis, Probab. Theory Rel. Fields **103**, 199 (1995).
[21] J. Krug and H. Spohn, in *Solids Far From Equilibrium*, edited by C. Godrèche, (Cambridge University Press, Cambridge, England, 1992).
[22] L.-H. Tang, B. M. Forrest, and D. E. Wolf, Phys. Rev. A **45**, 7162 (1992); T. Ala Nissila *et al.*, J. Stat. Phys. **72**, 207 (1993).